Chin. J. Astron. Astrophys. Vol. 5 (2005), No. 2, 211–220
(*http://www.chjaa.org*)

Chinese Journal of
Astronomy and
Astrophysics

DEFPOS and Its First Results

M. Şahan[1], İ. Yeğingil[1], N. Aksaker[1], Ü. Kızıloğlu[2] and M. Akyılmaz[1]

[1] Department of Physics, Çukurova University, 01330, Adana, Turkey
msahan2000@yahoo.com
[2] Department of Physics, Middle East Technical University, Ankara, Turkey

Received 2004 September 28; accepted 2004 December 1

Abstract A spectrometer was built to examine the interstellar medium (ISM) using the hydrogen Balmer α line. It is called Dual Etalon Fabry-Perot Optical Spectrometer (DEFPOS). DEFPOS will be coupled to coudé exit of the 150 cm telescope (RTT150) installed at TÜBİTAK National Observatory (TUG). DEFPOS was ready for observations about two years ago, but work was still continuing on the RTT150 coudé exit alignment. So we have started observing HII regions with DEFPOS without the RTT150. We present here some characteristics of the instrument and some of the results obtained.

Key words: ISM: general – ISM: HII regions – instrumentation: Interferometers – techniques: interferometric – atmospheric effect

1 INTRODUCTION

Interstellar medium (ISM) plays a fundamental role in the process of galactic evolution. This process involves a complex interplay between interstellar matter and stars. The stars are born from interstellar matter. During their lives, they deposit energy into the ISM in the form of electromagnetic radiation and stellar winds. When they die, they return some of their matter and energy back into the ISM. More massive stars do this in dramatic supernova events. The matter returned to the ISM is enriched with heavy elements produced by the nuclear burning in the stars' interior and in processes occurring during the explosions. This enriched ejecta becomes the material for future generations of stars which behave rather differently due to the presence of the metals. The process is not 100% efficient; some of the matter remains locked up forever in compact objects such as white dwarfs, neutron stars and black holes. Therefore, the composition of a galaxy slowly proceeds from all ISM to no ISM. The chemical evolution of the galaxy results from this cycle of stellar birth, death, and enriched rebirth. The growth in the quantity of heavy elements allows, along the way, the possible formation of planets, rocks, and in at least one case living organisms (Reynolds 1997; Tufte 1997; Ferrière 2001).

The main components of ISM have been identified, but the structure is still largely a mystery. The galaxy consists of primarily hydrogen (90%), some helium (10%), and only trace

quantities of heavier elements (Spitzer 1978; Dopita & Sutherland 2002). The gaseous component of the ISM is known to contain regions of atomic hydrogen (HI regions), molecular hydrogen (H_2), and ionized hydrogen in the form of classical HII regions, a warm diffuse component (10^4 K), and a hot component (10^6 K) (McKee & Ostriker 1977; Haffner et al. 1999). Diffuse, ionized gas component of the interstellar medium (sometimes also referred to as the Diffuse Ionized Gas: DIG or Reynolds Layers), plays an important role in the complex stellar-interstellar matter and energy cycle. This has been known over 30 years, since the discovery of the pulsars and the dispersion on their radio pulses by the free electrons that have been stripped from the atomic hydrogen along the line of sight (Reynolds 1997; Tufte 1997). Within a few kpc of the Sun this ionized gas is characterized by regions of nearly fully ionized hydrogen, a temperature near 10^4 K, having an electron density of 0.1 cm^{-3}, and occupying 20% or more of the volume within a 2 kpc (1 pc= 3.086×10^{13} km) thick layer about the Galactic mid-plane. The mass of the HII is approximately 1/3 that of the HI, and the required power is equal to that from the supernovae, making this gas a major component of the interstellar medium. The source of this ionization still remains, however, a mystery, and a challenge to conventional wisdom on the ISM and the principal mechanisms of ionization and heating within the disk and halo of our Galaxy (Reynolds 2002; Ferrière 2001).

Fabry-Perot type spectrometers are used for the detection of faint optical emission lines (like HII, SII, NII, OIII) from this diffuse ionized gas in the disk and halo of the Galaxy. The well known advantage of the Fabry-Perot spectrometer is that of at a specific spectral resolving power it has a throughput 100 to 200 times larger than that of a grating spectrometer with a same size dispersing element. This advantage is achieved because, compared to the grating, the Fabry-Perot can accept light from a much larger solid angle. The resulting large field of view therefore makes the Fabry-Perot well suited for spectral analysis of faint, spatially extended sources. Moreover, with the subsequent development of low read noise and high quantum efficiency CCDs (Charge Coupled Devices) in recent years, the efficiency of Fabry Perot spectrometers have been increased considerably (Reynolds et al. 1990; Yeğingil et al. 2004). In addition to velocity-resolved studies, large-area imaging surveys are also in progress. Gaustad et al. (2001) have completed a robotic wide-angle imaging survey of the southern sky (δ= +15° to –90°) at 656.3 nm wavelength with arcminute resolution. Moreover, the northern sky with 1.6 arcminute resolution has been continuing by using Virginia Tech's Spectral Line Imaging Camera (SLIC) (Dennison et al. 1998).

One of the Fabry-Perot type spectrometer is the WHAM (Wisconsin H-Alpha Mapper). WHAM consists of a 15 cm aperture, a dual etalon Fabry-Perot spectrometer coupled to a 0.6 m siderostat designed to study faint optical emission lines from diffuse sources at high spectral resolution. This spectrometer has surveyed the distribution and kinematics of ionized gas in the Galaxy above declination –30° in the Balmer-α line of hydrogen (Hα) emitted from ISM. The WHAM survey comprises more than 37000 individual spectra of the one degree beam in 30 second integration time (Haffner 2003). The calibrated spectra and velocity interval maps are available and can be downloaded from the WHAM website (www.wham.astro.wisc.edu). A similar instrument called DEFPOS has started observations at TÜBİTAK National Observatory (TUG) (Antalya/Bakırlıtepe) in Turkey in November of 2002. Both instruments are designed to detect Hα emission from HII regions in ISM and emission from other emission lines from the ionized gas, such as SII, NII and OIII. Characteristics of DEFPOS are given in a subsequent sections.

2 DEFPOS

In 1975, a spectrometer called PEPSIOS (Poly Etalon Pressure Swept Interferometric Optical Spectrometer) was built (Yeğingil 1978; Yeğingil et al. 1980) at the Physics Department of Middle East Technical University (METU, Ankara). At that time, since there was no suitable telescope in Turkey to be used with it to observe ISM, it was used to examine telluric absorption of sodium in the upper atmosphere and its structure (Yeğingil 1978).

The location of TUG has been selected by careful reconnaissance of potential regions in Turkey. Site testing observations made between 1982 and 1986 and a comparison of different locations shows Bakırlıtepe to be an outstanding site. It has further been shown that the location of TUG compares very favorably with the Raque de los Muchachos Observatory on la Palma, one of the world's best site observatories (Aslan et al. 1989). The latitude and longitude of TUG are 36° 51′ and –30° 20′, and the elevation is 2547 m.

After TUG was established in 1996, a 150 cm telescope has been installed. The telescope has a coudé focus, so a spectrometer can be coupled to it. Then it has been decided to build a similar instrument to WHAM and to couple it to the 150 cm telescope. The result is DEFPOS. In the construction we have used some old parts of PEPSIOS, such as the frame (etalon chambers), the etalon plates, etalon holders, etc. A CCD holder and a computer controlled pressure control system have been designed and constructed that controls the pressure of the chambers within ±1 mBar precision. The imaging CCD that was in TUG, a Loral LICK3 2k×2k back illuminated tinned and AR coated CCD, resides in an Infrared Labs Dewar. A San Diego State University controller sits on the Dewar and is connected to a control card in a Sun Ultra 1 computer via fiber-optic communications cable. The CCD chip is cooled with liquid nitrogen (LN_2) to a temperature of about –110 °C. The size of the CCD is $30 \times 30\,\mathrm{mm}^2$ and the pixel size is $15 \times 15\mu\mathrm{m}^2$.

DEFPOS was designed to be used in the coudé room of the telescope. However, the coudé exit of telescope can only be completed and made available at the end of the summer of 2004 while DEFPOS was ready for observation already in November 2002. So, we set up it in a room on the upper floor of the telescope building and through a hole on the ceiling. Observations have been carried out in the zenith direction. Similar work will be continuing till the coudé exit of telescope is ready. With the present set up of the spectrometer there is no pre-etalon optics, the instantaneous field of view (IFOV) of the spectrometer is 4.76°. This field of view will be reduced to 4′ when DEFPOS is used at the coudé focus. Some instrumental parameters of WHAM and DEFPOS are given in Table 1 for comparison. As is clearly seen in the table, with the present set up both the spectral and spatial resolutions of DEFPOS are low compared to WHAM, but when it is coupled to the telescope the spatial resolution will be higher. So in order to compensate for the high spatial resolution, the spectral resolution has been reduced. It is also important to note that the radius of the Fabry-Perot etalons used in DEFPOS is half the radius used in WHAM. In the future, if it is needed, the theoretical spectral resolution of the spectrometer will be increased to around 35 000.

Figure 1 shows a sketch of DEFPOS and its instrumental diagram. As can be clearly seen in the figure, light from the zenith first passes through a narrow-band interference filter (∼15 Å FWHM at Hα) in order to eliminate the unwanted parasitic light and to limit the observed spectrum. Then, it passes through the 7.5 cm aperture dual etalon Fabry-Perot etalons located in the pressure chambers. Finally, the light passes through the ring imaging lens that is placed just after the etalons in order to focus the ring image onto a 2.1 cm^2 region of the CCD chip. As the figure shows, there is no pre-etalon optics so the desire for about a 260 km s^{-1} spectral

Table 1 A comparison of DEFPOS and WHAM systems. The last column shows the properties of DEFPOS when it is used with the telescope. Then, the theoretical spectral resolution is planned to be 35 000, so in all respects it will be comparable with WHAM except that DEFPOS spatial resolution will be much higher.

	WHAM	DEFPOS	DEFPOS coupled with telescope
Diameter of the Etalon	15 cm	7.5 cm	7.5 cm
CCD	1024×1024 24μm $\times 24\mu$m pixels (QE=88%)	2086×2048 15μm $\times 15\,\mu$m pixels (QE=88%)	2086×2048 15μm $\times 15\mu$m pixels (QE=88%)
FOV	1°	4.76°	$4'$
Integration time	30 s	1200 s	< 60 s
$R_{\rm T}$ (theoretical)	43 000	19 000	35 000
$R_{\rm E}$ (experimental)	25 000	11 000	-
Telescope to be used with	Siderostat with 63 cm diameter lens	no pre-etalon optics	telescope
Gas used for pressure control	SF_6 ($n = 1.00072$)	N_2 ($n = 1.00027$)	SF_6 and N_2
Filter (FWHM)	20 Å Hα	15 Å Hα	15 Å Hα

interval requires a 2.38° half angle for the cone of rays passed through the etalons (Şahan 2004), and in the DEFPOS system the imaging CCD detector simultaneously records both the Fabry-Perot ring pattern and an image of the sky (Fig. 4a). Each annular ring on the detector corresponds to a particular spectral interval, but in this system the amount of light reaching the ring on the detector is now determined by the corresponding spatial ring on the sky. Hence an ambiguity exists: a bright spot on the detector may indicate either a spectral feature, a spatial feature, or some combination of the two (Tufte 1997). However, since we are interested in the integrated light at the end the spectrum by taking annular summing is constructed, then this ambiguity is removed. When the telescope is used with DEFPOS we will use pre-etalon optics to couple the telescope to the spectrometer, then there will be no such spectral and spatial mixing.

3 DATA REDUCTION

CCD images were acquired by imaging the ring pattern by the double-etalon Fabry-Perot interferometer onto the CCD chip. Standard CCD data reduction procedure has been used to reduce the data. The procedure is summarized in the following paragraphs. Besides data images there are three more CCD images which are taken for each observing night for reducing the data images (the "data" hereinafter), for bias, dark count and flat field. The first step when processing the images is to remove hot pixels produced by cosmic rays from all the images.

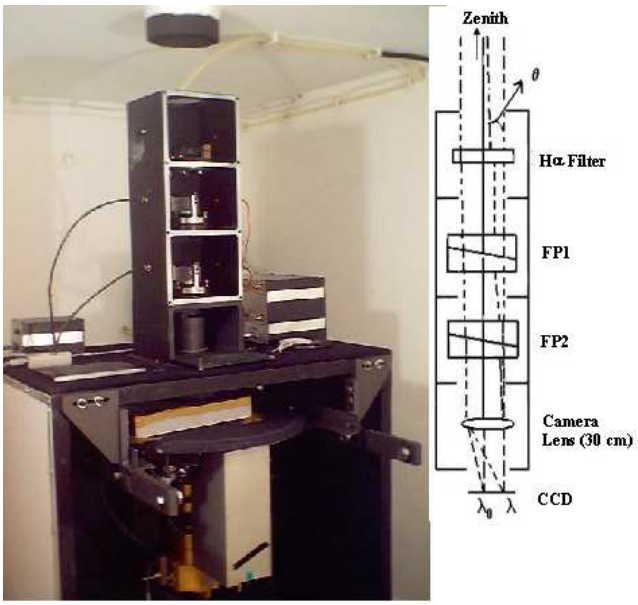

Fig. 1 DEFPOS (a) is shown in the observing room. The door of the pressure chambers is left open so that the filter and etalons in their holder can be seen. A diagram of the instrument (b) is also given. The dashed lines denotes the path of the light through the system. For details see the text.

Most cosmic ray hits produce signals which are one or two orders of magnitude brighter than those produced by the geocorona and they are removed with the three sigma (3σ) neighbour rejection criterion. After all the hot pixels have been removed, bias is removed from the three images (data, dark count and flat field) just by subtracting it. Next the dark count is subtracted from the flat field and data. All the above operations are done pixel by pixel. After the data is divided by the white light flat field to compensate for vignetting and for variations in pixel to pixel sensitivity on the CCD chip, the image is ready to be used to produce the line profile. The data image is converted into a line profile through an annular summing procedure. This is based on the principle that equal area annuli corresponds to equal wavelength (or wavenumber) intervals on the Fabry-Perot ring pattern. First the center of individual Fabry-Perot ring pattern is determined and then the image is ring summed (Coakley et al. 1996; Şahan 2004).

We have used a curve fitting software to fit Gaussians to the observed data. For each observed line separate Gaussians were used, and for the geocoronal line only one Gaussian was used. This has been enough for all cases. For the Galactic line sometimes more than one Gaussian is needed with different widths and heights to obtain the best fit. The position and the approximate line width of the geocoronal line are known. The area of the Gaussians which gave the best fit to the data is then used to determine the intensity of both the geocoronal Hα line and the Galactic Hα line. The curve fitting procedure tries to get the best fit by varying the height and the line widths of both the geocoronal and Galactic lines. WHAM data taken from WHAM's web site have been used for intensity calibration. DEFPOS' IFOV is 4.76°, and since the spectrometer works in the zenith direction with a 20 minutes integration time, DEFPOS' IFOV sweeps 9.00° so the observed FOV of the instrument is 9.00° by 4.76°. This implies that

DEFPOS' FOV sees around 30 WHAM's FOVs during the 20 minute integration period. To find the observed intensity for DEFPOS by using WHAM intensity results, we chose some test FOVs that DEFPOS had observed, and determined the same region in the WHAM data. Then, by sweeping 4.76° FOV through 9.00° over WHAM intensity data and adding the intensity values, we define the intensity value that DEFPOS should observe (Haffner et al. 2003). As a result of this calibration procedure it has been found that 20 ADUx (km s^{-1}) corresponds 1 R for the DEFPOS measurement near Hα. Preliminary calibration has been made and the detailed calibration method has been under progress (Şahan 2004). In order to test the obtained intensity value, we chose four test region with angular size equal to the FOV of DEFPOS and calculate the observed intensity by using (1) the calculated intensity value (20 km s^{-1}) and (2) the WHAM intensity data. One of the test results is given in Fig. 2, showing (a) an Hα CCD image and (b) a spectrum obtained after the annular summing. The (4.76° × 9.00°) observed region is centered at $b = -14.28°$ and $l = 88.55°$. This observation was made on 2003 June 27, between 01:15 to 01:35 UT. The intensity obtained from the calculated value is 5.43±1.09 R and the intensity obtained from the WHAM data is 7.62 ±1.52 R. Within the experimental error the intensity calibration of DEFPOS is good and acceptable. In our calculation the IFOV sweeps 9.00° during observation so it is impossible to exclude the Hα intensities from starlight. We include the Hα intensities from stars which have been removed from the original WHAM data (more information about the WHAM data can be found in 'The data use documents' which is accessible from *www.wham.astro.wisc.edu/wham*).

4 RESULTS AND DISCUSSION

DEFPOS work started on 2002 October 30, and from then on, observations have been made on 37 nights during dark moon in order to avoid contaminations of the reflected sunlight. An integration time of 1200 seconds is used in order to achieve signal to noise (S/N) ratios of greater then 10 for the line whose brightness is 0.5 R near Hα. For the geocoronal Hα line the S/N is higher because of its greater brightness. In this study it has been found that the intensity of the geocoronal line changed from 2 R to 15 R depending on the solar shadow height. During the observation period we have collected a total of 545 spectra near 6563 Å. DEFPOS has been primarily designed to observe ISM, but since the spectrometer observes through the earth's atmosphere the geocoronal hydrogen is automatically observed as a by-product. The IFOV of the spectrometer sweeps the sky during observation resulting in an FOV of 4.76° × 9.00° on the sky. Figure 3 shows the movement of the IFOV's center during the observation on the night of 2003 September 28. On that night, on the line of sight there was a bright structure known as the California Nebula (see Fig. 3). The CCD image and the spectrum of this nebula are shown in Fig.4. The CCD image shows that the ring is not uniformly illuminated by the source. The bright region on the CCD image is the result of the spatial feature of the nebula. This is because the spectrometer does not have a pre-etalon so it records both spectrum of the source and image of the sky at the same time. However, once the spectrum is taken based on the annular summing method this ambiguity can be removed. Two different structures are seen on the spectrum, marked 1 and 2. Line 1 shows the geocoronal Hα and line 2 indicates the galactic structure near Hα. The intensity of the observed Galactic line is 35.5±7.10R. The corresponding EM is 79.87 ±15.97 cm^{-6} pc, and the brightness of Hα emission from geocorona is 7.24±1.45R.

It is the first time that both Galactic Hα and geocoronal Hα intensity data are observed at this latitude (36° 51′N and –30°20′ E). The data span over only one year, so cannot be

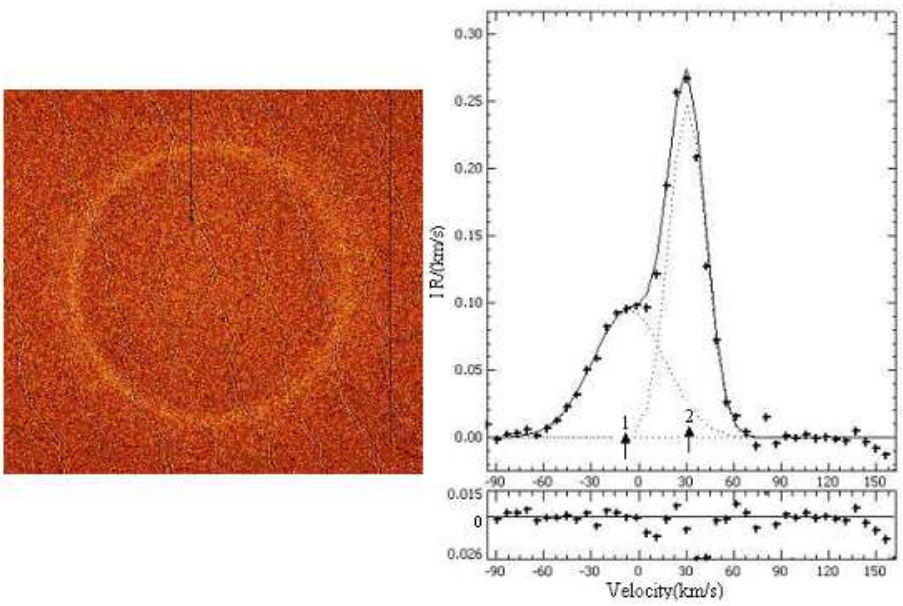

(a) (b)

Fig. 2 DEFPOS CCD image (a) and the spectrum obtained by annular summing procedure (b). The center coordinate of the observed region ($4.76^\circ \times 9.00^\circ$) is $b = -14.28^\circ$ and $l = 88.55^\circ$. This observation was made on 2003 June 27 between 01:15 to 01:35 UT. Galactic emission intensity (denoted as 1) is 5.43±1.09 R. The narrow and bright feature (denoted as 2) at 30.6 km s^{-1} is Hα emission from the geocorona and its intensity is 7.24±1.38 R.

used to look for long term tends in the exospheric emissions. Long term measurements of Hα intensities, however, can be used to predict long term trends which may be arisen due to the increase in greenhouse gases in the lower atmosphere. Changes in methane over the period considered in some works have resulted in a predicted exospheric hydrogen increase of about 10%. Observations of these upper boundary conditions can be used in assessing the degree to which models concerned with environmental perturbations in the lower atmosphere are accurately addressing coupled effects in other regions of the atmosphere. So accumulating geocoronal Balmer α intensities for a long period of time may be useful in detecting increases of greenhouse gas in the lower atmosphere (Nossal 1994).

A primary contamination in our DEFPOS data arises from the geocoronal Hα emission line profile. It is emitted in the Earth's upper atmosphere by scattering solar Lyβ radiation ($n = 1 \rightarrow 3$). The intensity of this line ranges from 2 to 13 R. Since the intensity of the exciting scatter Lyβ depends most sensitively on the height of the earth's shadow along the line of sight, the strength of the contamination line depends on the time and direction of the observation. Thus, in zenith direction with a constant declination and hour angle, the intensity of the geocoronal line changes from a minimum at midnight to a maximum at twilight by a factor of 3 or 4 (see Fig. 5). Since the Earth's orbital velocity changes the location of the velocity frame of the local standard of rest (LSR) with respect to the geocentric velocity frame, directions in the sky must be observed when the geocoronal line is separated from the LSR.

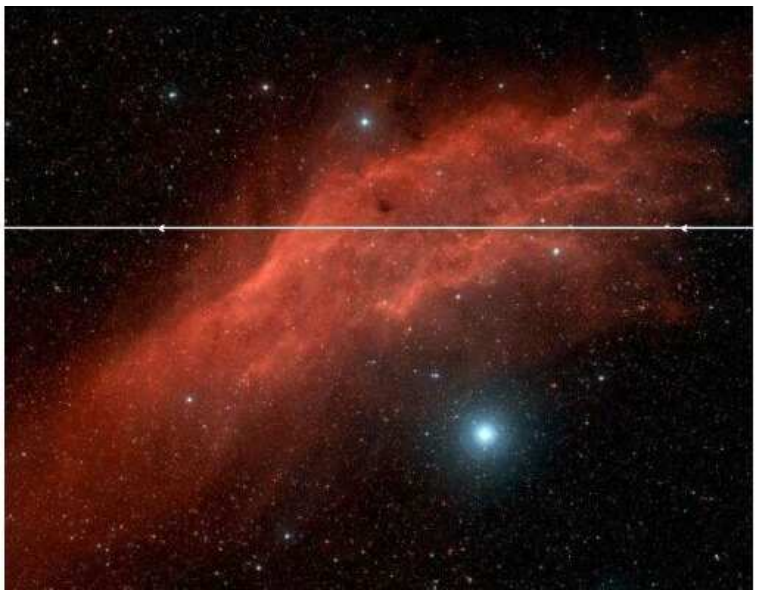

Fig. 3 The California Nebula that was observed on 2003 September 28. The line indicates the center of moving IFOV (Image size: $2.9^\circ \times 2.3^\circ$).

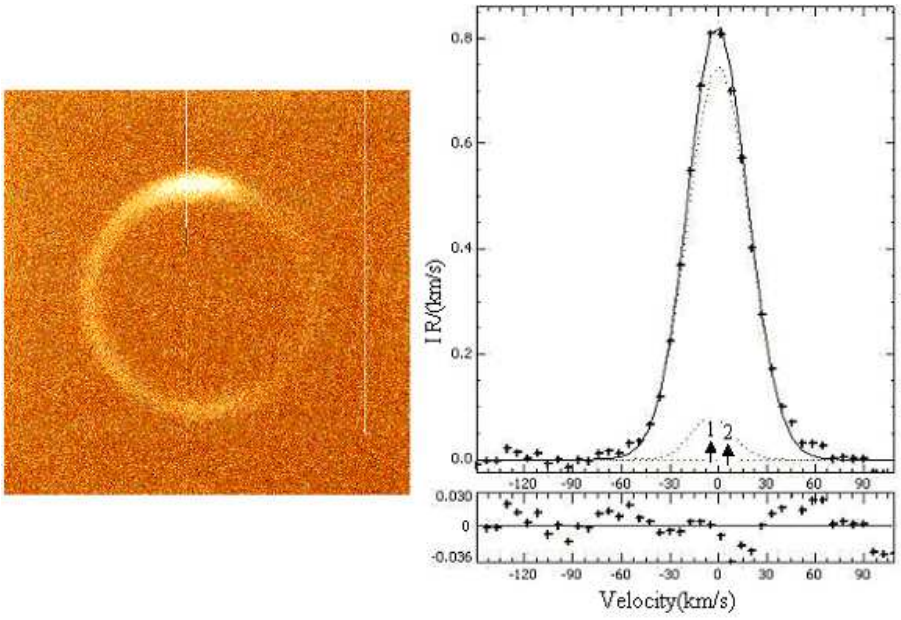

(a) (b)

Fig. 4 A CCD image (a) and its spectrum (b). Observation was made on 2003 November 22 around 10:02 UT. The center of the observed FOV in 1200 s integration time is $b = -10.38^\circ$, $l = 161.81^\circ$. Intensity of galactic and geocoronal lines are respectively 35.5 ± 7.10 R (1) and 7.24 ± 1.45 R (2).

Unfortunately, our only opportunity is to observe in the zenith direction and we do not have the opportunity of examining data at a variety of viewing geometries. To analyze the Galactic Hα emission and extract the geocoronal emission from our individual data, we must know precisely the shape of each line to be subtracted. In order to remove geocoronal Hα emission line from the galactic Hα emission line, we fit each individual sky spectrum and then subtract the resulting geocoronal Gaussian component from the raw Hα data. The LSR velocity parameter is used to determine the location of the geocoronal line, and it is exact enough in the time and direction of all observations. This provides the location of the geocoronal Hα line that has been removed from the spectrum. In the LSR velocity frame the geocoronal line was centered at (–VLSR−2.33) km s^{-1}. Then the DEFPOS spectra are velocity calibrated by our fits to this geocoronal line present in each observation. The geocoronal Hα line is characterized by a single Gaussian at our spectral resolution and is easily fitted and removed from all the galactic profiles. Thus we obtained individual galactic and geocoronal Hα lines.

Figure 5 shows the intensity variation of the geocoronal Balmer α line during the night of 2003 September 28. A quadratic is fitted to the data, shown in the figure. The geocoronal Hα line intensity measurements showed a change from 2 to 12 R. Figure 5 gives the intensity variation of an observed geocoronal Hα line at a time when the Galactic line was quite faint. The resolution of DEFPOS is 11 000 which corresponds to an instrumental line width of 30 km s^{-1} (0.65 Å) and the line width of the geocoronal Hα line is around 10 km s^{-1}, so it is impossible to determine the temperature of the geocoronal hydrogen line, but the intensity can be defined (Haffner 1999).

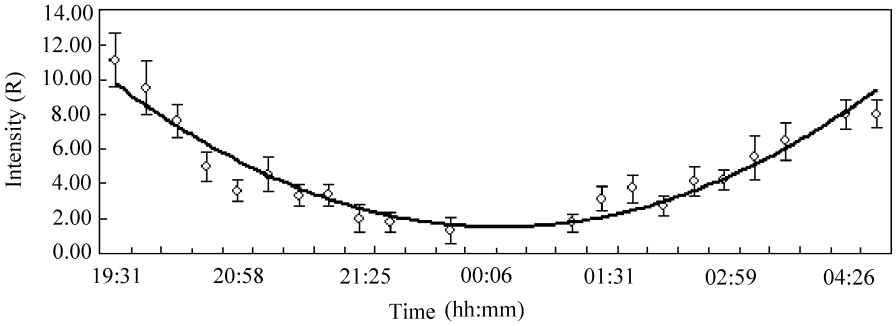

Fig. 5 Time variation of the geocoronal Balmer α intensity variation as a function of time observed on the night of 2003 September 28.

5 CONCLUDING REMARKS

DEFPOS, a 7.5 cm dual-etalon Fabry-Perot spectrometer with spectral resolution around 30 km s^{-1}, was designed to carry out HII observations by detecting Hα emission from selected regions of Galactic ISM in the northern sky. It was to be used in the coudè room of the 150 cm telescope at TUG. In its primary spectral mode, DEFPOS will sample the sky with 4 minutes of arc or smaller angular resolution. Because of the delay with the coudè exit of the telescope, DEFPOS has been set up in a room in the telescope building. Through a hole in the ceiling DEFPOS has been used to observe in the zenith direction with a 4.76° FOV. It will be moved to coudè room as soon as the coudè exit of the telescope is ready. Then we will

start observing ISM with $4'$ spatial resolution. The spectral resolution of the instrument may be altered as necessary. This will be done by simply changing the spacers of the etalons. The spacers that we have been using at the moment are 198 μm and 148 μm.

DEFPOS will be used to investigate some of the interesting HII regions in the Milky Way Galaxy with a lower angular resolution than WHAM. Besides interstellar work, DEFPOS will be used to observe the geocorona to examine the state of hydrogen and its variation. Long term measurement of the geocoronal Hα intensities can also be carried out to predict long term trends in the variation of greenhouse gas in the lower atmosphere.

Acknowledgements This project has been supported by Çukurova University, Middle East Technical University, Sabancı University and TUG (TÜBİTAK National Observatory). WHAM, the Wisconsin H-Alpha Mapper, is funded by the National Science Foundation, USA.

References

Aslan Z., Aydın C., Tunca Z. et al., 1989, A&A, 208, 385

Coakley M. M., Roesler F. L., Reynolds R. J., Nossal S., 1996, Appl. Opt., Vol. 35, No. 33, 6479

Dennison B., Simonetti, J. H., Topasna G. A., 1998, Publ. Astron. Soc. Australia, 15, 147

Dopita M. A., Sutherland R. S., 2002, Astrophysics of the Diffuse Universe, Heidelberg: Springer, Kapitel 11 (Bibliothek des Astronomischen Instituts)

Ferrière K. M., 2001, Rev. Mod. Phys., 73, 1031

Gaustad J. E., McCullough P. R., Rosing W., Van Buren D., 2001, PASP, 113, 1326

Haffner L. M., Reynolds R. J., Tufte S. L., 1999, ApJ, 523, 223

Haffner L. M., 1999, PhD Thesis, University Of Wisconsin, Madison

Haffner L. M., Reynolds R. J., Tufte S. L. et al., 2003, ApJS, 149, 405

McKee C. F., Ostriker J. P., 1977, ApJ, 218, 148

Nossal S., 1994, PhD Thesis, University Of Wisconsin, Madison

Reynolds R. J., Roesler F. L., Scherb F., Harlander J., 1990, In: D. Crawford, ed., Instrumentation In Astronomy VII, (Bellingham: SPIE), 610

Reynolds R. J., 1997, Science, 277, 1446

Reynolds R. J., Haffner L. M., Madsen G. J., 2002, In: M. Rosado, L. Binette, L. Arias, eds., ASP Conf. Ser., Vol. 282, Galaxies: The Third Dimension, p.31

Roesler F. L., 1974, Methods of Experimental Physics, Academic Press. Inc. Part 12., Vol. 12

Spitzer L. Jr., 1978, Physical Processes in The Interstellar Medium, New York: Willey-Interscience

Şahan M., 2004, PhD. Thesis, University Of Çukurova, Adana, Turkey

Tufte S. L., 1997, PhD. Thesis, University Of Wisconsin, Madison

Yeğingil İ., 1978, PhD. Thesis, Middle East Technical University, Ankara, Turkey

Yeğingil İ., Ögelman H., Kızıloğlu Ü., 1980, J. Geophys. Res., 85, C10, 5507

Yeğingil İ., Kızıloğlu Ü., Şahan M. et al., 2004, The Magnetized Interstellar Medium, Uyaniker B., Reich W., Wielebinski R., eds, Copernicus GmbH, Katlenburg-Lindau, p.227